Chinese Chemical Letters 33 (2022) 1946–1950

Contents lists available at ScienceDirect

Chinese Chemical Letters

journal homepage: www.elsevier.com/locate/cclet

Blood-based Alzheimer's disease diagnosis using fluorescent peptide nanoparticle arrays

Leming Sun*, Yang Lei, Yuerong Wang, Dingchang Liu

Key Laboratory of Space Bioscience and Biotechnology, School of Life Sciences, Northwestern Polytechnical University, Xi'an 710072, China

ARTICLE INFO

Article history:
Received 10 August 2021
Revised 20 October 2021
Accepted 24 October 2021
Available online 30 October 2021

Keywords:
Self-assembly
Alzheimer's disease
Fluorescent peptide nanoparticles
Blood-based diagnosis
Tau proteins
Multimodal

ABSTRACT

There is a critical need to diagnose and monitor the progression of Alzheimer's disease (AD) using blood-based biomarkers. At present, it is believed that tau biomarkers can be utilized to reliably detect AD. Multimodal techniques are highly sought after for AD diagnosis and progression monitoring. For this purpose, we developed a fluorescent peptide nanoparticles (f-PNPs) arrays that is capable of detecting multiple signals simultaneously. The concentration, aggregation stages, and Young's modulus of tau biomarkers could be analyzed by monitoring the changes of multimodal fluorescence intensity, nano-morphological, and nano-mechanical properties of the f-PNPs arrays. Experimental results indicated that, compared to healthy human, the concentration, Young's modulus, and aggregation levels of tau proteins in blood samples of clinically diagnosed AD patients increased continuously with the increase of disease severity. The minimally invasive and multimodal characterization techniques showed high signal-to-noise ratio for AD diagnosis.

Despite the increasing prevalence of Alzheimer's disease (AD) and the significant efforts towards developing novel diagnostics, sensitivity and specificity of current AD detection approaches are still far less reliable [1–3]. Given the absence of effective diagnostic approaches, significant concerns have been raised regarding current treatment trials and management strategies. Blood-based AD diagnosis has been eagerly pursued for AD detection owing to the ease and low cost of acquisition, a large number of analytes contained within it, and its suitability for the preclinical population-based screening of patients over the age of 50 years [4–6]. Although the diagnosis of AD using blood-based biomarkers would be significant, no reliable blood-based test is available now [7,8]. The disease is difficult to diagnose, as deteriorating cognitive abilities are often detected once it is too late.

The rapid development of new blood-based diagnostic procedures and recent advances in protein chip technologies are driving the development of AD diagnosis [9,10]. However, the complexity of these chips also raises many challenges along with a high cost to manufacture [11–13]. For example, enzyme-linked immunosorbent assays (ELISA) applied to analyze the concentration of biomarkers inside human blood can only use the monoclonal antibody as matched pairs, which are costly and difficult to find [14,15]. In addition, negative controls may indicate positive results if the blocking solution is ineffective. Recent AD diagnostics, like magnetic resonance imaging and positron emission tomography, are either expensive or lack sufficient accuracy to tease apart AD pathology from changes associated with normal aging [16–18]. Moreover, it is difficult to distinguish AD from other dementias and monitor the progression of AD.

Lab-on-a-chip technology provides an advantage to improve diagnosis efficiency [19]. Chip-based technologies have several advantages over conventional bio-analysis systems, such as rapid analysis of a large number of samples in a single experiment, reagent economy, and the signal-to-noise ratio exhibited by the chips is much better than that observed for conventional assays [20]. Furthermore, lab-on-a-chip technology has significant advantages in regulating microenvironments and integrating with automation systems that are critically needed for controlling peptide self-assembly to achieve specific sequences and nanostructures. On the other hand, the use of peptides for constructing selective functional nanostructures has many applications as functional components for lab-on-a-chip devices towards specific demands. Peptides have demonstrated their exceptional benefits in developing self-assembled nanostructures and devices with expected functionalities [21–24]. The diversity of the amino acids for peptide sequence design allows feasibility for developing multi-functional nanomaterials [25–28]. Recently, we made many progresses on fabricating fluorescent dipeptide nanoparticles for detecting specific AD protein biomarkers [29–32]. Different from the conventional array-

* Corresponding author.
E-mail address: lmsun@nwpu.edu.cn (L. Sun).

https://doi.org/10.1016/j.cclet.2021.10.071
1001-8417/

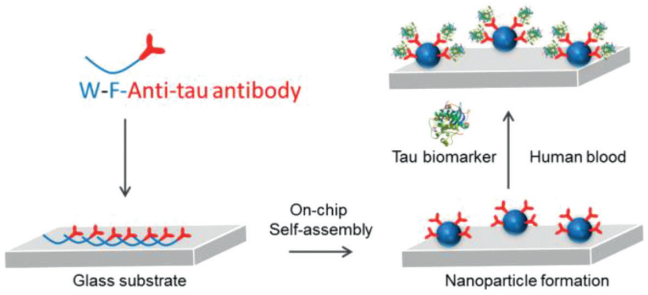

Fig. 1. Self-assembly of anti tau f-PNPs arrays on glass substrate through on-chip self-assembly to detect tau biomarkers from human blood.

based detection, this study presents fluorescent peptide nanoparticles (f-PNPs) arrayed microfluidic chips that allow multimodal detection. As hallmarks of AD development, tau proteins are one of the most commonly assayed AD protein biomarkers to clinically diagnosis and monitor the progression of AD as their concentration, Young's modulus, and morphological aggregation levels are closely related to the disease progression [33–36]. In this study, tau proteins from human serum have been detected and analyzed as a proof-of-concept in the aspects of multimodal fluorescent, nano-morphological, and nano-mechanical changes under the same tightly controlled microenvironment, in terms of sample control, data acquisition, and analysis. To correlate these biomarkers in a more comparable manner for AD diagnosis, the fluorescence intensity, Young's modulus, and morphological aggregation levels of the f-PNPs array upon targeted binding with biomarkers were measured to quantitatively diagnose and monitor the progression of AD.

Detailed experiment procedures are shown in supporting information. The normal role of the tau protein is to keep the cytoskeleton well organized in the axonal process. However, in AD it is ineffective because this protein loses its capacity to bind to microtubules. This abnormal behavior is promoted by conformational changes and misfolding in the normal structure of tau that leads to its aberrant aggregation into fibrillar structures inside the neurons of demented individuals. Thus, as one of the principal hallmarks of AD, tau is also viewed as a good diagnostic and predictive biomarker. In this study, synthetic tau protein aggregates with concentrations of 10 and 100 ng/mL were prepared and utilized. The anti tau f-PNPs self-assembled with anti-tau antibody at the surface of the nanoparticles (Fig. 1). There were peaks of fluorescence emission at around 420 nm from the anti tau f-PNPs arrays (Fig. 2A). It was observed from the peptide self-assemblies that there were single layer spherical nanoparticles with a diameter of approximately 10 nm. Based on the DHM (Digital holographic microscopy) image (Fig. 2C) of anti tau f-PNPs arrays, it can be seen that no obvious aggregates were observed, and the height of arrays was low. DHM is a potent tool to perform three-dimensional imaging and tracking for nanostructures. The Young's modulus of anti tau f-PNPs was around 200 MPa. Afterwards, tau proteins with concentrations of 10 and 100 ng/mL were controlled to flow through anti tau f-PNPs arrays and dried at room temperature. We hypothesize that, due to the anti tau antibody at the surface of f-PNPs, functional anti tau f-PNPs would recognize and bind with tau proteins. Consequently, fluorescence intensity, Young's modulus, and morphological aggregation levels of anti tau f-PNPs could be characterized based on interacting with different concentration of tau proteins to validate the blood-based AD diagnosis and progression monitoring.

After interacting with synthetic tau, the fluorescence intensity of anti tau f-PNPs decreased as seen in the fluorescent spectrum in Fig. 2A. Most importantly, the fluorescence intensity of anti tau f-PNPs decreased more when binding with more synthetic tau proteins. With increased concentration of synthetic tau proteins, there is more decrease in fluorescence intensity. The interaction of f-PNPs with tau protein could also alter fluorophores and quench the fluorescence of f-PNPs. The decrease of fluorescence intensity indicates interactions between anti tau f-PNPs and tau proteins. The greater the concentration of tau proteins, the greater the quenching as more proteins are present at the surface of f-PNPs. In Fig. 2B, the f-PNPs treated with tau proteins of concentrations 10 and 100 ng/mL have similar values of around 60 MPa. The higher Young's modulus of the anti tau f-PNPs could be due to the peptide sequences. The different Young's modulus values between anti tau f-PNPs and synthetic tau proteins could be utilized for the detecting of tau proteins through the nano-mechanical characterizations using the lab-on-a-chip devices. The nano-morphological results in Fig. 2C also showed that, after interactions with different amounts of synthetic tau proteins, the aggregation levels of anti tau f-PNPs changed. The AFM and DHM images showed that aggregation levels increased with increasing concentration of synthetic tau proteins. These results are consistent with the fluorescent results in Fig. 2A. With an increase in synthetic tau protein aggregates, there could be more chances to bind at the surface of anti tau f-PNPs, thereby inducing more tau aggregation and fluorescent intensity decrease. The fluorescence intensity and aggregation levels (Fig. 3) of f-PNPs arrays without any recognition sites after binding with synthetic tau proteins aggregates showed no significant difference, which indicated the specific binding between anti tau f-PNPs and tau proteins. This study proved the detecting capacities of the anti tau f-PNPs chips for tau proteins. Through detecting tau proteins in human blood samples, these chips could be further utilized to diagnose and monitor the progression of AD.

The deposition of aggregated tau proteins into neurofibrillary tangles and neurotic tau pathology is one of the hallmarks in AD. Alterations in the amount or the structure of tau proteins can affect the stabilization of microtubules and other processes related to AD [37]. Therefore, anti tau f-PNPs arrays had blood samples from AD patients and healthy human controlled to flow through them and dried at room temperature in order to verify blood-based diagnosing and monitoring the progression of AD. The serum was obtained from a total of 32 human subjects, ranging from 54 to 83 years of age ($n = 8$, healthy; $n = 8$, mild AD; $n = 8$, moderate AD; $n = 8$, severe AD; all based on clinical diagnosed information). All the research related to human subjects was received and approved by the Medical Ethics Committee of Northwestern Polytechnical University (2019–05). All volunteers were noticed and agreed for the participation. The detail of the gender and age of the subjects are listed in Table S1 (Supporting information). The resulted fluorescence, nano-morphological, and nano-mechanical properties of the f-PNPs arrays should be different upon binding with tau protein aggregates in serum samples. As shown in Fig. 4A, anti tau f-PNPs arrays treated with serum from healthy human had obvious intensity drops. In addition, the massive conjugation between f-PNPs and tau protein aggregates in serum led to more loss of fluorescence signal from f-PNPs arrays treated with serum from AD patients. Among the AD patients, the fluorescence intensity decreased more and more with an increase in disease severity from mild to moderate to severe AD cases. Combined with the results in synthetic tau proteins, the higher amount of intensity decrease could be due to the increased amount of tau protein aggregates detected in serum samples. Therefore, the results confirmed that, as the disease severity increases from healthy to severe AD patients, the concentration of tau proteins aggregates in serum increases.

The nano-mechanical characterization data in Fig. 4B showed that, as disease severity ranges from healthy human to AD patients in different stages, the Young's modulus of tau protein aggregates in serum is different. Compared to patients with AD, the

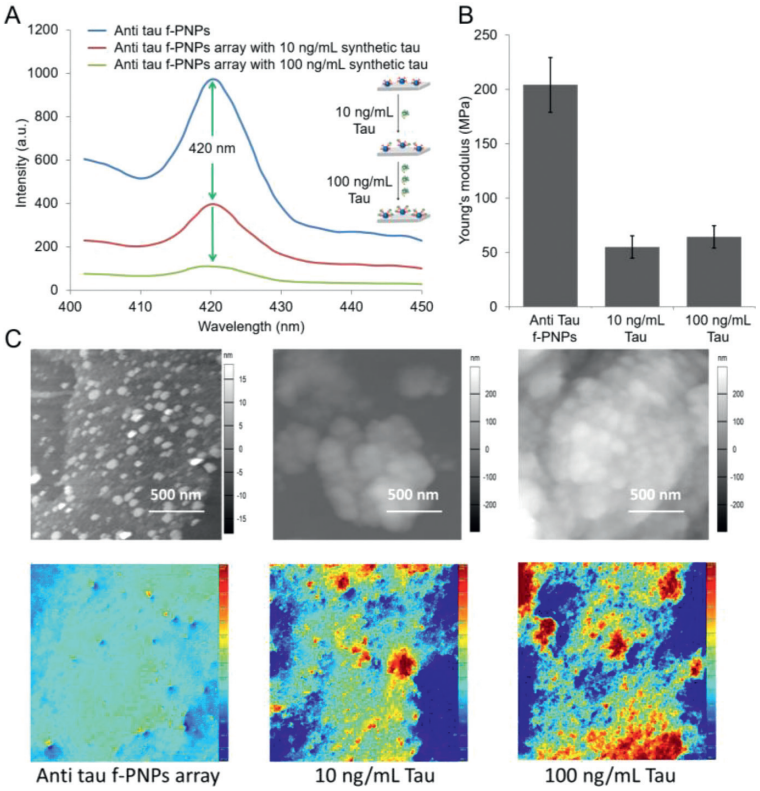

Fig. 2. Multimodal fluorescence intensity, nano-morphological, and nano-mechanical changes of anti tau f-PNPs array treated with different concentrations of synthetic tau proteins. (A) Solid state fluorescence emission spectra of anti tau f-PNPs array before and after binding with 10 and 100 ng/mL synthetic tau proteins. (B) The Young's modulus of anti tau f-PNPs array before and after binding with 10 and 100 ng/mL synthetic tau proteins. (C) AFM and DHM images of anti tau f-PNPs array treated with synthetic tau proteins.

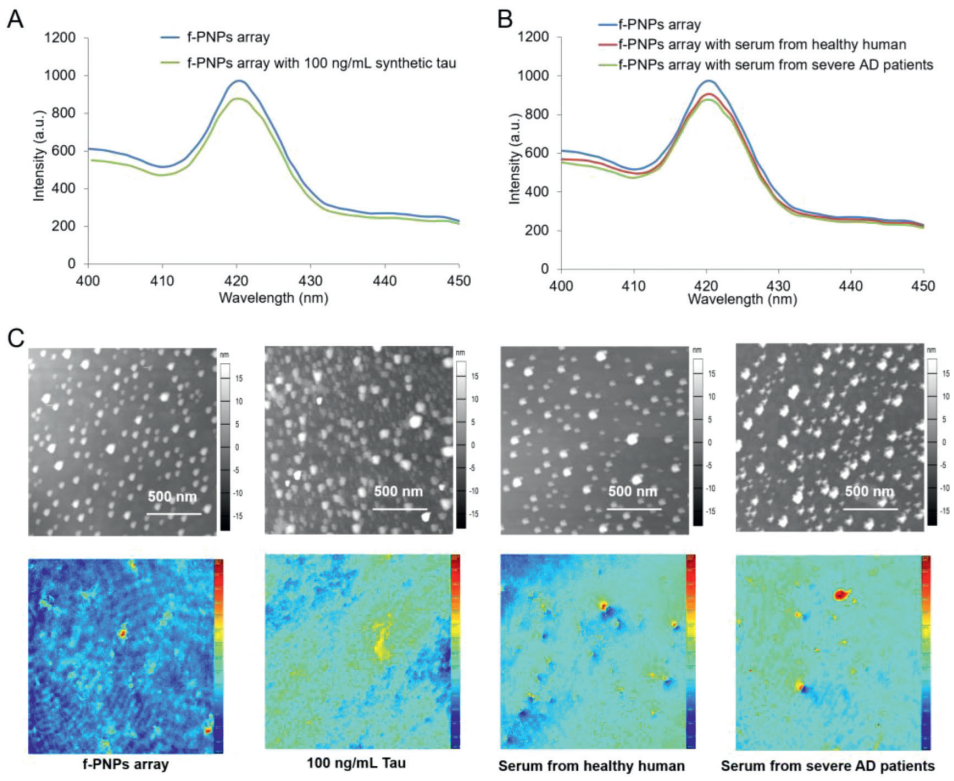

Fig. 3. Fluorescence intensity and nano-morphological changes of f-PNPs array treated with different concentrations of synthetic tau proteins and serum from healthy human and severe AD patients. (A) Solid state fluorescence emission spectra of f-PNPs array before and after binding with 100 ng/mL synthetic tau proteins. (B) The Young's modulus of f-PNPs array before and after binding with serum from healthy human and severe AD patients. (C) AFM and DHM images of f-PNPs array treated with synthetic tau proteins and serum from healthy human and severe AD patients.

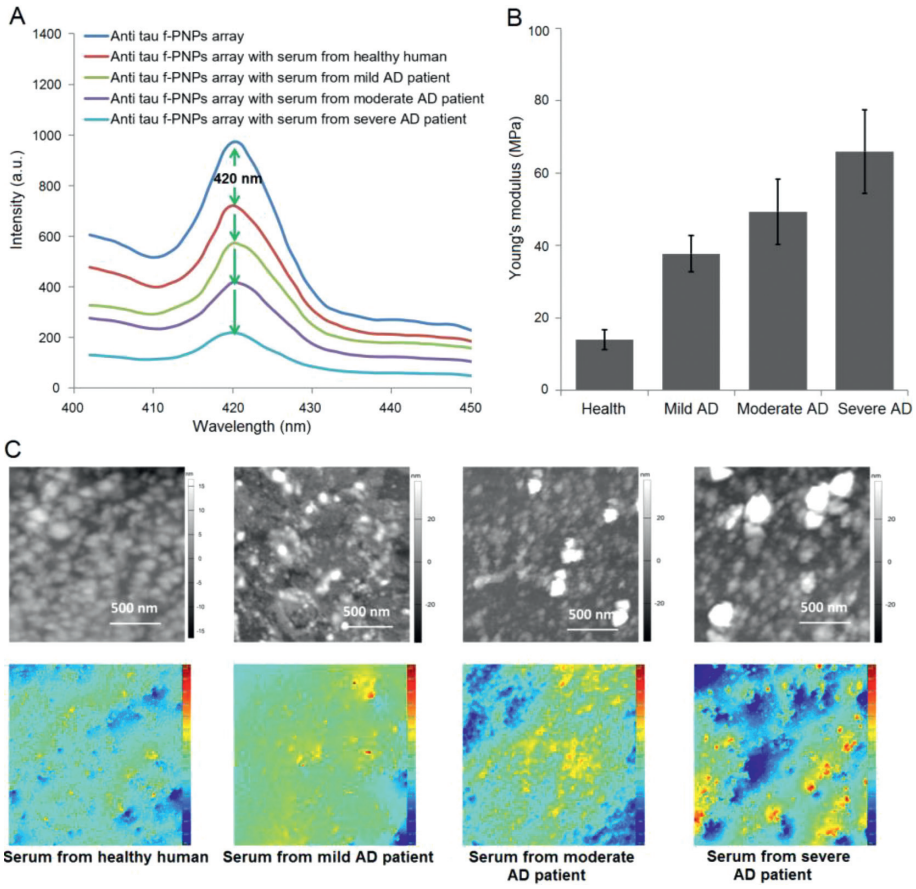

Fig. 4. Multimodal fluorescence intensity, nano-morphological, and nano-mechanical changes of anti tau f-PNPs array treated with serum from healthy human and AD patients with different stages. (A) Solid state fluorescence emission spectra of anti tau f-PNPs array before and after binding with tau proteins in serum from healthy human and AD patients. (B) The Young's modulus of anti tau f-PNPs array before and after binding with tau proteins in serum from healthy human and AD patients. (C) AFM and DHM images of anti tau f-PNPs array treated with tau proteins in serum from healthy human and AD patients.

lowest value of Young's modulus, which is only around 14 MPa, occurs in the healthy human. The Young's modulus of f-PNPs conjugated tau protein aggregates increases as disease severity increases from mild (38 MPa) to moderate (50 MPa) to severe AD (65 MPa) patients. The increasing stiffness of the protein aggregates results from an internal change that takes place in the structure of tau proteins. During the progression of AD, the structure and density of tau proteins are different. It is mostly accepted that abnormal post-translational modifications, that is, hyperphosphorylation, acetylation, glycation, nitration, and truncation are responsible for altered tau structures in AD. The detection capabilities of the Young's modulus of tau protein aggregates in human blood samples also proved that the f-PNPs arrays could be used to diagnose and monitor the progression of AD using nano-mechanical characterization. The Young's modulus of tau proteins in serum from healthy human and AD patients with varying stages are different when compared to those of synthetic tau protein aggregates at different concentrations. However, each of these is able to induce and affect different fluorescence intensity changes. These discoveries indicated that the detection results could be affected by not only concentration, but also by the aggregation levels or structures of the tau protein aggregates. Therefore, the concentration and aggregation levels of tau proteins in serum from healthy human and AD patients with different stages could be used as the detecting standards for the diagnosis and progression monitoring of AD. The nano-morphological property data in Fig. 4C showed that, after the interaction with tau protein aggregates in serum from healthy human and AD patients with varying stages, the aggregation levels of anti tau f-PNPs were different. Compared with healthy human, both AFM and DHM images showed that AD patients had increased aggregation levels of f-PNPs conjugated tau protein aggregates. Furthermore, with increasing severity of patients from mild to moderate to severe cases, the aggregation levels of tau proteins in serum also continuously increased. These results are consistent with the above fluorescent and nano-mechanical observations in that the structure or aggregation levels of tau protein aggregates are different from healthy human and AD patients with varying stages, which could be utilized to diagnose and monitor the progression of AD.

In this study, a new type of f-PNPs arrays were designed and fabricated for multimodal diagnosis and progression monitoring of AD using serum from healthy human and AD patients. Multimodal characterization techniques including fluorescent, nano-morphological, and nano-mechanical properties were applied to do the data extraction. Compared with healthy human, the concentration and aggregation levels of tau proteins in blood samples from AD patients are higher, which induced higher fluorescence intensity decreases through fluorescence quenching effects. In addition, the decreased level of fluorescence intensity, Young's modulus, and aggregation levels of the f-PNPs arrays after interacting with tau proteins in blood continuously increased with the increase of disease severity from mild to moderate to severe AD patients. The increase of the Young's modulus was due to the growth of complex internal structure and density inside tau proteins in serum from healthy human to AD patients with the increase of disease sever-

ity. We believe that the simplicity, sensitivity, and selectivity of this assay would make it potentially suitable for the clinical diagnosis and progression monitoring of AD.

Declaration of competing interest

The authors declare that they have no known competing financial interests or personal relationships that could have appeared to influence the work reported in this paper.

Acknowledgments

This work was supported by the National Natural Science Foundation of China (No. 31900984), the Natural Science Basic Research Plan in Shaanxi Province of China (No. 2019JQ-231), the China Postdoctoral Science Foundation (No. 2018M631197), the Shaanxi Postdoctoral Science Foundation (No. 2018BSHQYXMZZ42), the Fundamental Research Funds for the Central Universities (No. 31020180QD063). We would like to thank the Analytical and Testing Center of Northwestern Polytechnical University for the AFM characterization.

Supplementary materials

Supplementary material associated with this article can be found, in the online version, at doi:10.1016/j.cclet.2021.10.071.

References

[1] H. Hampel, R. Frank, K. Broich, et al., Nat. Rev. Drug Discov. 9 (2010) 560–574.
[2] C. Bastin, E. Salmon, Eur. J. Clin. Nutr. 68 (2014) 1192–1199.
[3] P. Yang, C. Yang, K. Zhang, et al., Chin. Chem. Lett. 29 (2018) 1811–1814.
[4] D.M. Chuang, H.K. Manji, Biol. Psychiatry 62 (2007) 4–6.
[5] C. Rodriguez, E. Albanese, A. Pegna, et al., Dement. Geriatr. Cogn. Disord. Extra 6 (2016) 120–132.
[6] H. Zeng, Y. Qi, Z. Zhang, et al., Chin. Chem. Lett. 32 (2021) 1857–1868.
[7] T. Kasai, T. Tokuda, M. Taylor, et al., Neurosci. Lett. 551 (2013) 17–22.
[8] C. Lausted, I. Lee, Y. Zhou, et al., Annu. Rev. Pharmacol. Toxicol. 54 (2014) 457–481.
[9] J.E. Anderson, L.L. Hansen, F.C. Mooren, et al., Drug Resist. Updates 9 (2006) 198–210.
[10] P. Miao, Y. Tang, B. Wang, et al., Anal. Chem. 88 (2016) 7567–7573.
[11] C. Sheridan, Nat. Biotechnol. 23 (2005) 3–4.
[12] V. Romanov, S.N. Davidoff, A.R. Miles, et al., Analyst 139 (2014) 1303–1326.
[13] C. Timm, C.M. Niemeyer, Angew. Chem. Int. Ed. 52 (2013) 2652–2654.
[14] T. Yang, S. Hong, T. O'Malley, et al., Alzheimers Dement. 9 (2013) 99–112.
[15] N. Xia, X. Wang, B. Zhou, et al., ACS Appl. Mater. Interfaces 8 (2016) 19303–19311.
[16] K.E. Pike, G. Savage, V.L. Villemagne, et al., Brain 130 (2007) 2837–2844.
[17] Y. Li, Y. Huang, Z. Wang, et al., Small 12 (2016) 668–677.
[18] C.M. Clark, J.A. Schneider, B.J. Bedell, et al., JAMA J. Am. Med. Assoc. 305 (2011) 275–283.
[19] C.D. Chin, V. Linder, S.K. Sia, Lab Chip 7 (2007) 41–57.
[20] J. Workman, M. Koch, D. Veltkamp, Anal. Chem. 77 (2005) 3789–3806.
[21] L. Sun, A. Li, Y. Hu, et al., Part. Part. Syst. Charact. 36 (2019) 1800420.
[22] Y. Liu, D. Li, J. Ding, X. Chen, Chin. Chem. Lett. 31 (2020) 3001–3014.
[23] W. Ma, S. Sha, P. Chen, et al., Adv. Healthc. Mater. 9 (2020) 1901100.
[24] H. Zhang, S. Dong, Z. Li, et al., Asian J. Pharm. Sci. 15 (2020) 397–415.
[25] D. Fu, D. Liu, L. Zhang, L. Sun, Chin. Chem. Lett. 31 (2020) 3195–3199.
[26] Z. Yu, Q. Xu, C. Dong, et al., Curr. Pharm. Des. 21 (2015) 4342–4354.
[27] W. Lin, Y. Yang, Y. Lei, et al., ACS Appl. Mater. Interfaces 13 (2021) 32799–32809.
[28] K. Wang, W. Ma, Y. Xu, et al., Chin. Chem. Lett. 31 (2020) 3149–3152.
[29] L. Sun, D. Liu, D. Fu, et al., Chem. Eng. J. 405 (2021) 126733.
[30] Z. Fan, L. Sun, Y. Huang, et al., Nat. Nanotechnol. 11 (2016) 388–394.
[31] L. Sun, Z. Fan, T. Yue, et al., Bio-Des. Manuf. 1 (2018) 182–194.
[32] D. Liu, D. Fu, L. Zhang, L. Sun, Chin. Chem. Lett. 32 (2021) 1066–1070.
[33] K. Blennow, M.J. de Leon, H. Zetterberg, Lancet 368 (2006) 387–403.
[34] S. Rolstad, J. Jakobsson, C. Sellgren, et al., PLoS One 10 (2015) e0127100.
[35] K. Blennow, Expert Rev. Mol. Diagn. 5 (2005) 661–672.
[36] C. Humpel, Trends Biotechnol. 29 (2011) 26–32.
[37] H. Kadavath, R.V. Hofele, J. Biernat, et al., Proc. Natl. Acad. Sci. U. S. A. 112 (2015) 7501–7506.